Check for updates

Crystallization, thermal and mechanical properties of stereocomplexed poly(lactide) with flexible PLLA/PCL multiblock copolymer†

Zhanxin Jing, [iD] * Xiaolan Huang, Xinqi Liu, Mingneng Liao, Zhaoxia Zhang and Yong Li

In this work, the synthesized PLLA/PCL multi-block copolymers with different compositions were introduced into a stereocomplexed poly(lactide) (sc-PLA) matrix to accelerate the stereocomplexation of PLA enantiomers and improve its inherent brittleness. The PLLA/PCL multi-block copolymers were in different compositions to adjust the molecular weight of the PLLA block. The structure, molecular weight, crystallization behavior, crystal structure and thermal stability of PLLA/PCL multi-block copolymers were investigated. The results indicated that PLLA/PCL multi-block copolymers with controllable structure and composition were successfully synthesized. On this basis, the blends of sc-PLA and PLLA/PCL multi-block copolymers were prepared by solution casting, and characterized. The results revealed that the introduction of PLLA/PCL multi-block copolymers promoted the stereocomplexation of the PLA enantiomers during the melting crystallization process to obtain a complete stereocomplexed material. But the presence of the PCL block leads to a decrease in the melting temperature of the stereocomplex and difficulty in homogeneous nucleation. Compared with sc-PLA, the elongation at break of the blends was significantly improved and their tensile strengths were only slightly reduced. And the thermal stability and mechanical properties of the blends could be adjusted by controlling the content and composition of PCL/PLLA multi-block copolymers. These results revealed that the degree of stereocomplexation and toughness of sc-PLA were improved, which may expand the application fields of PLA-based materials.

1. Introduction

Poly(lactide) (PLA), which can be prepared by fermentation processes of carbohydrates and from plants (*e.g.* starch obtained from corn or sugar beet), is a completely biodegradable aliphatic polyester.[1,2] Due to its attractive mechanical properties, renewability, biodegradability and relatively low cost, PLA, its copolymers and blends have offered extensive potentials in many fields, such as medicine, food packing, textiles and agriculture.[3–5] At present, it is considered as an important candidate to replace petrochemical-based polymer materials to solve environmental problems and the shortage of petrochemical resources.[6] However, the inherent brittleness, slow crystallization rate and low impact strength of PLA represent the main limitations of sustainable industrial development.[7] Several strategies have been developed to improve these properties of PLA, such as copolymerization, blending with soft polymers or rubber-like polymers, chemical modification and adding additives. Recently, stereocomposite technology based on

stereochemistry has received extensive attention in the modification of PLA. PLA has three isomeric forms, namely, optically active poly(L-lactide) (PLLA) and poly(D-lactide) (PDLA), racemic poly(DL-lactide) (PDLLA), where PLLA and PDLA are semi-crystalline polymers and PDLLA is an amorphous polymer.[8] PLLA and its enantiomer PDLA are able to form the stereocomplexed poly(lactide) (sc-PLA), which is ascribed to the hydrogen bonding between L-lactyl and D-lactyl unit sequences.[9] Sc-PLA exhibits higher mechanical strength, higher melting point, higher heat distortion temperature, and faster crystallization rate with respect to the neat PLLA or PDLA.[10,11] To illustrate the formation mechanism of sc-PLA and discuss the crucial factors affecting its formation, many factors, such as molecular structure, molecular weight, optical purity, PLLA/PDLA mixing ratio, preparation method, and crystallization conditions have been studied.[12–14]

Recently, it has been studied that the degree of stereocomplexation can be improved by adjusting the structure of PLA. Cui *et al.*[15] investigated the influences of cross-linking agent and plasticizer on the formation and heat resistance properties of sc-PLA, found that the introduction of cross-linking agent and plasticizer significantly improves the heat resistance of sc-PLA, which is because the stereocomplexed (sc) crystallites were exclusively formed, excluding any homo-

Department of Applied Chemistry, College of Chemistry and Environment, Guangdong Ocean University, Zhanjiang, China. E-mail: jingzhan_xin@126.com

† Electronic supplementary information (ESI) available. See https://doi.org/10.1039/d2ra00461e

crystallization (hc) crystallites. Deng et al.[16] proposed an unprecedented strategy by one-pot reactive melt blending of the equimolar PLLA/PDLA blend with reactive poly(ethylene-methyl acrylate-glycidy methacrylate) to achieve the toughness of sc-PLA material and obtain exclusive sc-microcrystals in melt-processed products. The diblock copolymers based on PCL and PDLA/PLLA and the enantiomeric blends thereof along with a stereotriblock copolymer were synthesized by Mulchandani et al.[17] The results found that the incorporation of PCL significantly enhances the elongation at break of PLLA and PDLA. And the enantiomeric mixture is directly processed using injection molding process to produce cancellous bone screws, which have thermomechanical stability at 121 °C due to the stereocomplexation between the PLLA and PDLA blocks. Therefore, the synthesis of PLA-based copolymers with novel structures is an effective way to realize the toughening and full stereocomplexation of PLA enantiomers. Therefore, it is an effective way to expand the application of PLA to develop the technology to realize the full stereocomplex PLA-based materials.

However, the application of sc-PLA materials in more fields obviously is limited due to its weak melt memory effect in triggering complete sc-crystallization and inherent brittleness. The weak melt memory effect of sc-PLA often results in sc-crystallization accompanied with large hc-crystallization during melt processing, so the performance of the prepared product is far from that expected.[18,19] The introduction of stereocomplexed nucleating agents and the improvement of the mobility of polymer chains are considered to be effective methods for preparing fully sc-PLA-based materials. Hai et al.[20] designed a novel aryl hydrazide nucleating agent N,N,N,N'-salicylic tetra(1,2,4,5-benzenetetracarboxylic acid) hydrazide with plentiful hydrazide and hydroxyl groups and applied it to the crystallization of high molecular weight PLLA/PDLA blends, and found that the nucleating agent enhanced the crystallization rate and sc-crystallization ability of PLLA/PDLA blends by forming a large number of hydrogen bonds with the PLA chain. However, this method can only realize the stereocomplexation of PLLA/PDLA blends, but cannot improve its brittleness. Previous literature[21–23] have reported that the introduction of flexible polymer blocks can improve the toughness of sc-PLA materials. Purnam et al.[24] studied the stereocomplexation of PLLA and random copolymer of poly(D-lactide-co-ε-caprolactone) (PDLCL) with small content of ε-caprolactone, and found that the addition of small amount of caprolactone in the PDLCL is addressed as soft fragment to accelerate the movement of PDLA fragment to interact with PLLA chain. Sc-PLA-based materials were prepared by incorporating of poly(D-lactide)-b-poly(ethylene glycol)-b-poly(D-lactide) into the PLLA matrix.[25] The results showed that the tensile strength, elongation at break and heat resistance of the prepared PLA-based material can be improved, which is assigned to the synergistic effect of the stereocomplexation between the PLA enantiomers and the plasticizing effect of the poly(ethylene glycol) block.

In this study, the self-complementary quadruple hydrogen bonding between UPy groups was first used to construct PLLA/PCL multiblock copolymer (MBC). Then, the stereocomplex of PLLA and PDLA (sc-PLA) in the presence of PLLA/PCL

multiblock copolymers was prepared by the solution casting. Chemical structure and molecular weight of PLLA/PCL multiblock copolymers were measured by ^{1}H NMR and GPC, respectively. Their crystallization behaviors, crystal structures and thermal stability were also analyzed. Eventually, the properties of sc-PLA/MBC blends are studied in depth by WAXD, DSC, POM, TGA and tensile test.

2. Experimental section

2.1. Materials and reagents

L-Lactide and D-lactide (optical purity > 99%) were purchased from Jinan Daigang Biological Materials Co., Ltd., China. ε-Caprolactone was obtained from Beijing J&K Chemicals Co. Ltd, China. Stannous octoate ($Sn(Oct)_2$, >95%) and dibutyltin laurate (>95%) were purchased from Shanghai Macklin Biochemical Co., Ltd., China. A commercial poly(L-lactide) (4032) was supplied by American Nature Works Company. Poly(D-lactide) was synthesized by bulk ring-opening polymerization of D-lactide using $Sn(Oct)_2$ as the catalyst, and the number average molecular weight and polydispersity index of PDLA measured by GPC were 30.4 kg mol^{-1} and 1.31, respectively. 2-(6-Isocyanatohexylaminocarbonylamino)-6-methyl-4[1H]pyrimidinone (UPy-NCO) was synthesized according to the previous literature (in Fig. S1†),[26] using 2-amino-4-hydroxy-6-methylpyrimidine and 1,6-hexamethylene diisocyanate as raw materials, which were purchased from Beijing J&K Chemicals Co. Ltd, China. Other reagents were of analytical grade.
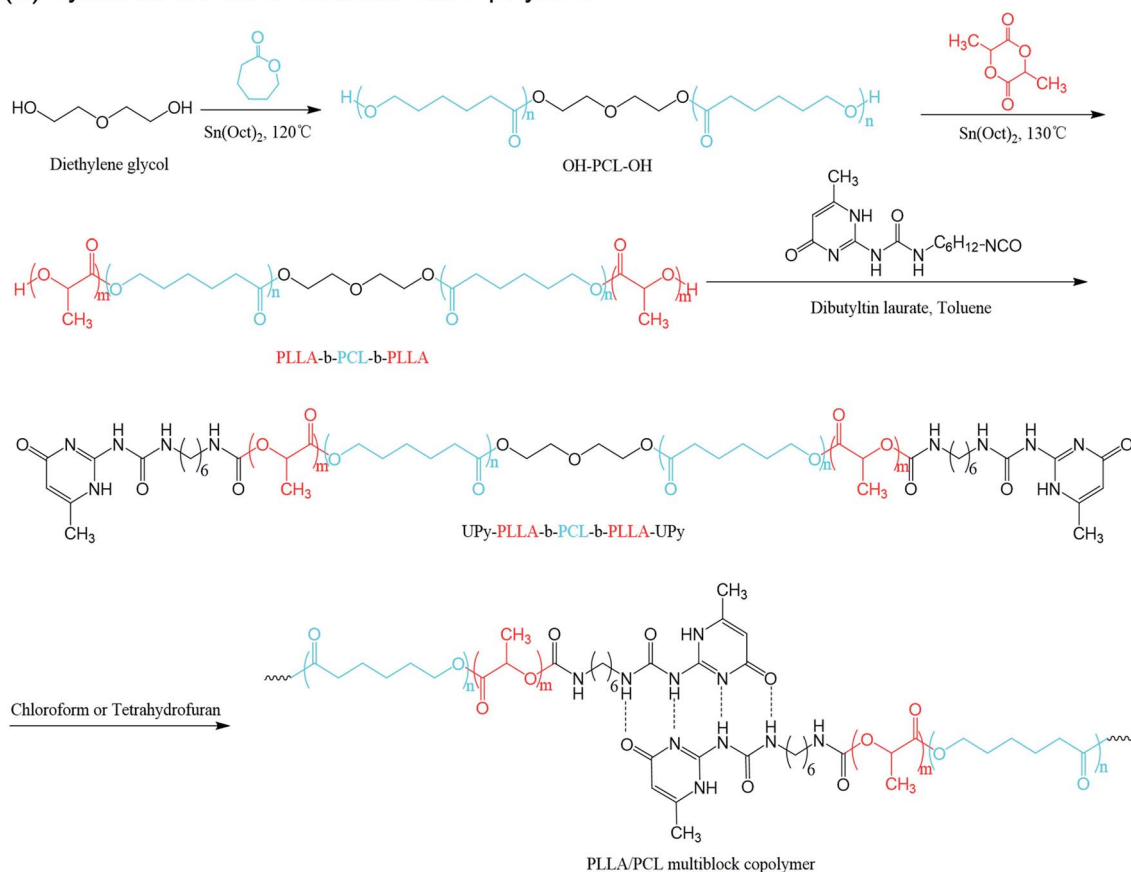
2.2. Synthesis of PLLA/PCL multiblock copolymers

PLLA/PCL multiblock copolymers were synthesized according to the previous literature,[27] as shown in Fig. 1. Firstly, the dihydroxyl functionalized poly(ε-caprolactone) (PCL) macroinitiator was synthesized. Diethylene glycol (0.16 g, 1.57 mmol) and ε-caprolactone (20.31 g, 177.94 mmol) were added to a 100 mL three-necked round-bottomed flask. After venting nitrogen to remove air, the mixture was heated to 120 °C, and the catalyst $Sn(Oct)_2$ was added. The amount of $Sn(Oct)_2$ is 0.1% of the molar amount of ε-caprolactone. After 24 h, the mixture was cooled to room temperature to stop the reaction, dissolved in dichloromethane and precipitated with methanol. The filtered precipitate was dried in a vacuum oven at 40 °C for 48 h, weighted and stored.

Afterwards, PLLA-b-PCL-b-PLLA triblock copolymers were synthesized by dihydroxyl functionalized poly(ε-caprolactone) macroinitiator to initiate ring-opening polymerization of L-lactide, using $Sn(Oct)_2$ as the catalyst. A certain weight of dihydroxyl functionalized poly(ε-caprolactone) macroinitiator and L-lactide were added to a three-necked round bottom flask, and vacuum was applied at 60 °C for 30 min to remove residual solvent and moisture. The mixture was heated to 130 °C, and stirred. 0.1% of $Sn(Oct)_2$ was added with respect to the molar amount of L-lactide. After 24 h, the mixture was cooled to room temperature, dissolved in dichloromethane, and precipitated with methanol. The precipitate was collected and dried in a vacuum oven at 40 °C for 48 h. The resulting product is labeled

(a) Synthesis of PLLA/PCL multiblock copolymers
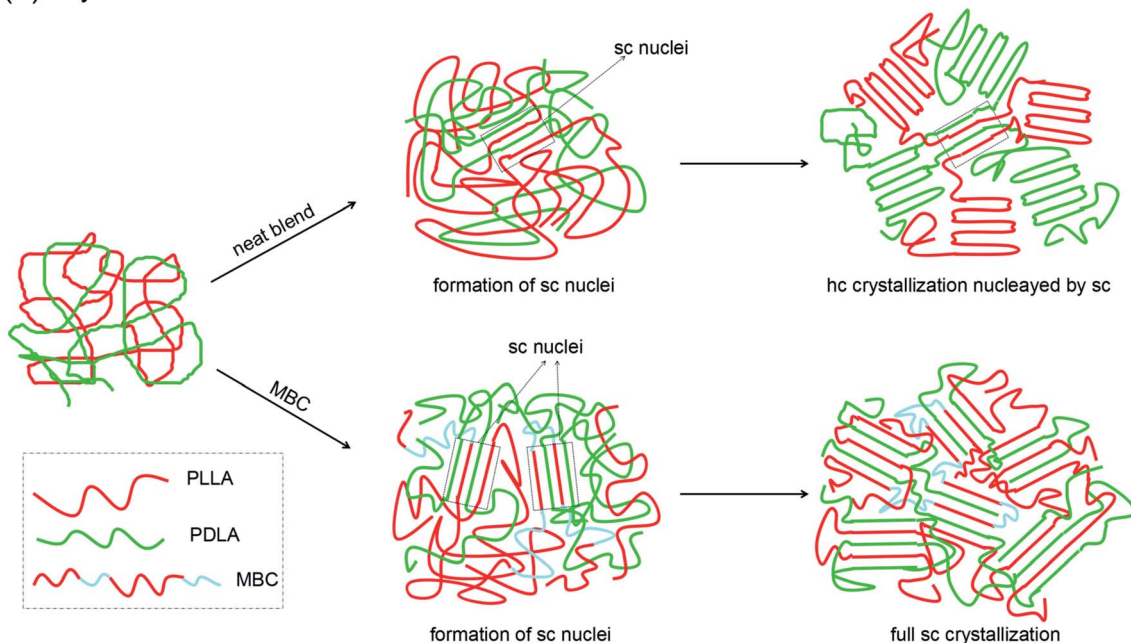

(b) Crystallization of PLLA and PDLA

Fig. 1 (a) Schematic diagram of the synthesis of PLLA/PCL multiblock copolymer based on PLLA-*b*-PCL-*b*-PLLA triblock copolymer; (b) crystallization of sc-PLA/MBC blends.

as TBC*X*, where *X* represents the molecular weight of PLLA block, calculated by ^{1}H NMR. The specific feeding ratios are listed in Table 1.

Eventually, PLLA/PCL multiblock copolymer was synthesized through the coupling reaction of PLLA-*b*-PCL-*b*-PLLA triblock copolymer and excess UPy-NCO. PLLA-*b*-PCL-*b*-PLLA triblock

Table 1 Composition and molecular weights of PCL macroinitiator, PLLA-*b*-PCL-*b*-PLLA triblock copolymer and PLLA/PCL multiblock copolymer

Samples	[LA]/[CL][a]	M_n of each block[b] (kg mol^{-1})	$M_{n,NMR}$[b] (kg mol^{-1})	$M_{n,GPC}$[c] (kg mol^{-1})	PDI[c]	m_{PLA}[b] (%)	Yield (%)
PCL	—	—	11.1	13.6	1.44	—	94.4
TBC0.9	1 : 4	0.9–11.1–0.9	12.9	14.6	1.22	14.0	75.7
TBC3.0	2 : 4	3.0–11.1–3.0	17.1	19.1	1.23	35.1	86.9
TBC5.0	3 : 4	5.0–11.1–5.0	21.1	23.0	1.21	47.4	89.3
MBC0.9	1 : 4	—	—	28.3	1.62	—	79.8
MBC3.0	2 : 4	—	—	39.8	1.65	—	71.8
MBC5.0	3 : 4	—	—	40.4	1.47	—	69.8

[a] [LA]/[CL] represents the mole ratio of the monomer lactide and caprolactone repeating unit in the PCL macroinitiator during the synthesis of PLLA-*b*-PCL-*b*-PLLA triblock copolymers. [b] Calculated from ^{1}H NMR results. [c] Measured by GPC.

copolymer (2.0 g) and UPy-NCO (1.0 g) were added to a 100 mL three-necked round bottom flask, and the vacuum was applied at 60 °C for 40 min to remove residual solvent. After filling with nitrogen, 50 mL of the dried toluene was added, and the mixture was heated to 110 °C. Next, 3.0 wt% of Sn(Oct)$_2$ was added with respect to PLLA-*b*-PCL-*b*-PLLA triblock copolymer. After 24 h, the mixture was filtered while hot, and the collected filtrate was concentrated by a rotary evaporator. The collected mixture was dissolved in 50 mL of chloroform, and 1.5 g of silica and 3 drops of dibutyltin dilaurate were added. The mixture was stirred at 60 °C for 1 h. After the reaction, the mixture was filtered to remove silica with UPy-NCO, and the filtrate was passed through a rotary evaporator to remove the solvent. The obtained product wad kept in a vacuum oven at 40 °C for 24 h, and was marked as MBC*X*, *X* represents the molecular weight of PLLA block in the PLLA/PCL multi-block copolymer.

2.3. Preparation of sc-PLA/MBC blends

Sc-PLA/MBC blends were prepared by solution casting. Firstly, equal weights of PLLA and PDLA were separately dissolved in chloroform (20 mL). At the same time, a certain weight of PLLA/PCL multi-block copolymer was dissolved in 10 mL of chloroform. The total weight of PLLA, PDLA and PLLA/PCL multi-block copolymers is approximately 1.0 g. Then, the above solutions were mixed, and stirred uniformly. The mixed solution was poured into a mold with diameter of 70 mm, and placed at room temperature to completely volatilize the solvent. Eventually, the obtained film was dried in a vacuum oven at 40 °C for 24 h. Sc-PLA/MBC blends with various MBC contents were labeled as sc-PLA/MBC-*Y*%, where *Y* represents the percentage of MBC3.0 in the sc-PLA/MBC blend and are set as 0%, 5%, 10%, 15% and 20%. Sc-PLA/MBC blends with different MBC*X* were marked as sc-PLA/MBC*X*, where the content of MBC in the blend was 15%.

2.4. Characterization

2.4.1. ^{1}H NMR. The ^{1}H NMR nuclear magnetic resonance (^{1}H NMR) spectra of the samples were measured by a Bruker 400 MHz NMR spectrometer in chloroform-*d* (CDCl$_3$). Tetramethylsilane (TMS) was used as a reference.

2.4.2. GPC. Number- and weight-average molecular weight (M_n, M_w) and polydispersity (PDI, M_w/M_n) of samples were

performed by gel permeation chromatography (GPC). Tetrahydrofuran (THF) was used as the mobile phase at a flow rate of 1.0 mL min^{-1}, and the fitting curve was established using monodisperse polystyrene standards.

2.4.3. WAXD. Wide angle X-ray diffraction (WAXD) patterns of the samples were performed on a Bruker D8 Advance X-ray diffractometer, using Cu Kα radiation as the incident X-ray beam. The 2θ angle ranged from 5° to 40° with a rate of 5° min^{-1} at room temperature.

2.4.4. DSC. Differential scanning calorimetry (DSC) was measured on a Q1000 instrument (TA Instruments) under nitrogen atmosphere according to the following conditions: the samples were first heated from 30 °C to 190 °C (or 240 °C) at the rate of 10 °C min^{-1}, and melted for 3 min to eliminate the thermal history; afterwards, the samples were cooled to 0 °C at a rate of 5 °C min^{-1}, and then heated to 190 °C (or 240 °C) at a rate of 10 °C min^{-1} again.

2.4.5. TGA. Thermogravimetric analysis (TGA) and differential thermogravimetric analysis (DTG) were measured by a Q500 instrument (TA Instrument). The samples were heated from 30 °C to 600 °C at a rate of 10 °C min^{-1} under nitrogen atmosphere.

2.4.6. POM. The crystalline morphology observations of the samples were performed on a polarizing microscope (POM, BK-POL, Chongqing Auto Optical Instrument Co., Ltd., China) equipped with a hot stage. The sample film was placed on a hot stage, heated to 250 °C, and melted for 3 min to eliminate thermal history. Afterwards, the molten substance was decreased to a predetermined temperature, and the change of spherulites growth with time was observed by POM.

2.4.7. Tensile test. Tensile properties were measured at room temperature by a mechanical tester, at a crosshead speed of 20 mm min^{-1}, using rectangular specimens with dimension of 30 × 3 × 0.1 mm^3. Each sample was tested six times to calculate the average value and deviation.

3. Results and discussion

3.1. Synthesis and characterization of PLLA/PCL multi block copolymers

Fig. 2(a) shows ^{1}H NMR spectra of PCL macroinitiator, PLLA-*b*-PCL-*b*-PLLA triblock copolymer and the corresponding PLLA/PCL multiblock copolymer. For PCL macroinitiator, there

exhibit several proton peaks at 1.4 ppm, 1.6–1.7 ppm, 2.4 ppm and 4.1 pm, assigned to the characteristic methylene proton signals of ε-caprolactone repeating units of PCL.[28] The proton corresponded to the terminal methylene group shows a weak peak at 3.7 ppm.[28,29] This suggests that the dihydroxy functionalized PCL macroinitiator was successfully synthesized. The number-averaged molecular weight ($M_{n,NMR}$) calculated by ^{1}H NMR is 11.1 kg mol^{-1}. The number-averaged molecular weight ($M_{n,GPC}$) of PCL was also determined by GPC (Fig. 2(b)), and there presents a peak on the GPC curve of PCL. It can be observed from Table 1 that the polydispersity index of PCL is 1.44, revealing that the distribution of molecular weight is narrow. The $M_{n,GPC}$ of PCL is 13.6 kg mol^{-1}, which is consistent with the result of ^{1}H NMR. In addition to the proton peaks of PCL, PLLA-*b*-PCL-*b*-PLLA triblock copolymer has obvious proton peaks at 1.57 ppm and 5.16 ppm, attributed to the methyl and methine protons of lactide units, respectively.[30] The methine protons next to the terminal hydroxy groups is observed at 4.36 ppm.[31] The $M_{n,NMR}$ of PLLA-*b*-PCL-*b*-PLLA triblock copolymers calculated by ^{1}H NMR are listed in Table 1. It is clear that the $M_{n,NMR}$ increases as the molar ratio of L-lactide to the repeating unites of PCL increases, which is consistent with the result of GPC (Table 1). And PLLA-*b*-PCL-*b*-PLLA triblock copolymer presents a low polydispersity index (<1.23). These results indicate that PLLA-*b*-PCL-*b*-PLLA triblock copolymer with controllable composition and molecular weight has been successfully synthesized.

For PLLA/PCL multiblock copolymer, it shows a ^{1}H NMR spectrum similar to the corresponding PLLA-*b*-PCL-*b*-PLLA triblock copolymer. However, three weak proton peaks were observed at 10.10 ppm, 11.85 ppm and 13.13 ppm, assigned to the characteristic proton peaks of the UPy groups.[27,32] GPC result also found that the molecular weight of PLLA/PCL multiblock copolymer is larger than that of the corresponding PLLA-*b*-PCL-*b*-PLLA triblock copolymer (Fig. 2(b)), which may be attributed to the formation of self-complementary quadruple hydrogen bonds between UPy groups (Fig. 1(a)). These results indicate that the PLLA/PCL multiblock copolymer based on PLLA-*b*-PCL-*b*-PLLA triblock copolymer are successfully synthesized.

3.2. Crystallization behavior, crystal structure and thermal stability of PLLA/PCL multiblock copolymers

Fig. 3(a) and (b) display DSC curves of PLLA-*b*-PCL-*b*-PLLA block copolymers and the corresponding PLLA/PCL multiblock copolymers, respectively. In Fig. 3(a), the cooling curve of TBC0.9 exhibits an obvious exothermic peak at 25.5 °C, assigned to the crystallization of PCL block. The corresponding reheating curve has double endothermic peaks at 49.8 °C and 55.3 °C, attributed to the melting of PCL crystal. The crystallization and melting peaks of PLLA are not detected, which may be due to the low molecular weight of the PLLA block. With increasing of the molecular weight of PLLA block, an exothermic peak is observed in the higher temperature region of the cooling curve, assigned to the crystallization of PLLA block. The corresponding reheating curve presents a melting peak of PLLA crystals, and the melting temperature shifts to the higher temperature region as the molecular weight of PLLA block increases. It is clear that in Fig. 3(b), the multi-block copolymer based on PLLA-*b*-PCL-*b*-PLLA triblock copolymer shows a similar curve to the corresponding PLLA-*b*-PCL-*b*-PLLA triblock copolymer. For MBC0.9, the temperature corresponded to PCL crystallization is obviously lower than that of TBC0.9 triblock copolymer, and the crystallization enthalpy of PCL is also smaller than the corresponding triblock copolymer (as Table 2). Other multi-block copolymers exhibit similar phenomena with respect to the corresponding PLLA-*b*-PCL-*b*-PLLA tri-block copolymers. As listed in Table 2, the crystallization temperature, melting temperature and enthalpy of all PLLA/PCL multiblock copolymers are smaller than those of the corresponding triblock copolymers. These results reveal that the PLLA/PCL multi-block copolymers have weaker crystallization ability than that of PLLA-*b*-PCL-*b*-PLLA triblock copolymers. The formation of self-complementary quadruple hydrogen bonds between UPy groups drives PLLA-*b*-PCL-*b*-PLLA triblock copolymer to form PLLA/PCL multi-block copolymer. This expands the polymer chain and increases its molecular weight, resulting in poor mobility of the polymer chain. Therefore, the multiblock copolymers based on PLLA-*b*-PCL-*b*-PLLA exhibits poor crystallization ability. Similar phenomena have been reported by Chang *et al.*[33] and Chen *et al.*[34]
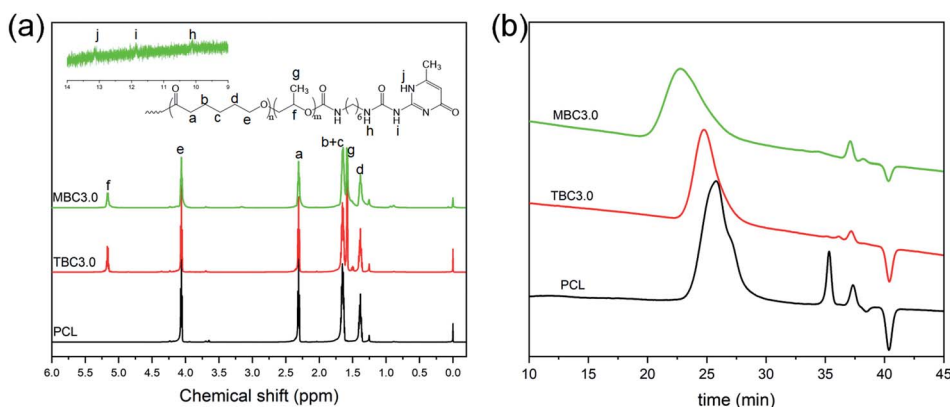

Fig. 2 ^{1}H NMR spectra (a) and GPC curves (b) of PCL, PLLA-*b*-PCL-*b*-PLLA triblock copolymer and PLLA/PCL multiblock copolymer.

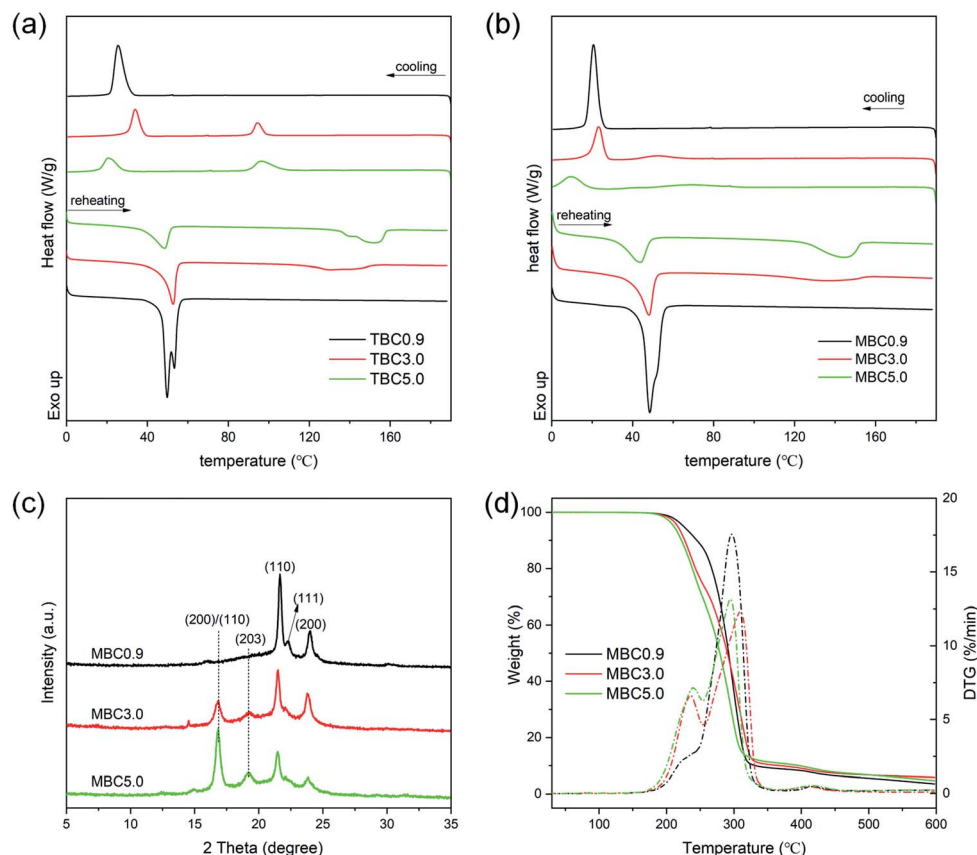© 2022 The Author(s). Published by the Royal Society of Chemistry

Fig. 3 (a and b) DSC cooling and reheating curves of PLLA-*b*-PCL-*b*-PLLA triblock copolymers (a) and the corresponding PLLA/PCL multiblock copolymers (b); (c) WAXD and (d) TGA curves of PLLA/PCL multiblock copolymers.

WAXD patterns of PLLA/PCL multi-block copolymers are shown in Fig. 3(c). For MBC0.9, there presents three characteristic diffraction peaks at 21.5°, 22.0° and 23.8°, attributed to the (110) and (111) and (200) planes of PCL crystals, respectively.[35] The diffraction peak of α crystal formed by the homo-crystallization of PLLA blocks is not detected. This may be attributed to the low molecular weight of the PLLA blocks, which is consistent with the result of DSC. With increasing of the molecular weight of PLLA block, there exhibit the obvious diffraction peaks at 16.5° and 18.7°, assigned to the (200)/(110) and (203) planes of α crystal formed by the homo-crystallization of poly(lactide), respectively.[36] It can be also observed that as the molecular weight of PLLA block increases, the diffraction peak corresponded to PCL crystals decreases, while the diffraction of PLLA crystals increases. This is mainly due to the change of the composition of PLLA/PCL multi-block copolymer. Fig. 3(d)

Table 2 Thermal parameters of PLLA-*b*-PCL-*b*-PLLA triblock copolymer and the corresponding PLLA/PCL multiblock copolymer obtained from DSC[a]

Samples	Cooling				Reheating			
	$T_{c,PCL}$	$\Delta H_{c,PCL}$	$T_{c,PLLA}$	$\Delta H_{c,PLLA}$	$T_{m,PCL}$	$\Delta H_{m,PCL}$	$T_{m,PLLA}$	$\Delta H_{m,PLLA}$
TBC0.9	25.5	67.8	—	—	49.8/55.3	67.6	—	—
TBC3.0	33.9	36.5	94.2	16.1	52.7	36.4	130.4/140.2	18.4
TBC5.0	25.6	23.6	96.3	26.5	48.5	24.6	140.9/151.8	26.4
MBC0.9	20.6	57.2	—	—	49.3	56.1	—	—
MBC3.0	23.1	29.5	52.3	7.8	48.1	29.0	135.4	11.4
MBC5.0	9.7	16.9	67.2	16.4	43.8	22.3	144.4	21.8

[a] $T_{c,PCL}$ (°C) and $\Delta H_{c,PCL}$ (J g^{-1}) denote the crystallization temperature and the corresponding enthalpy of PCL blocks in the cooling run; $T_{c,PLLA}$ (°C) and $\Delta H_{c,PLLA}$ (J g^{-1}) are the crystallization temperature and the corresponding enthalpy of PLLA blocks in the cooling run; $T_{m,PCL}$ (°C) and $T_{m,PLLA}$ (°C) are melting temperatures of PCL and PLLA blocks, respectively; $\Delta H_{m,PCL}$ (J g^{-1}) and $\Delta H_{m,PLLA}$ (J g^{-1}) are melting enthalpies of PCL and PLLA blocks, respectively.

presents TGA and DT curves of PLLA/PCL multi-block copolymers with various PLLA blocks. With increasing of the molecular weight of PLLA block, the onset temperature of degradation ($T_{5\text{ wt\%}}$) decreases from 225.3 °C to 210.9 °C. This reveals that the increase in the molecular weight of PLLA blocks leads to a decrease in the thermal stability of PLLA/PCL multi-block copolymers. This is because PLLA degrades at lower temperature with respect to PCL.[37] DTG curves of PLLA/PCL multi-block copolymers exhibit two sharper peaks of degradation at about 165–250 °C and 250–360 °C, assigned to the degradation of PLLA and PCL blocks, respectively. The presence of two degradation peaks also reveal that the PLLA/PCL multi-block copolymers exhibit two well-defined weight losses corresponding to the degradation of PLLA and PCL blocks.[38] In Fig. S2,† PCL and PLLA-*b*-PCL-*b*-PLLA triblock copolymer show poor film-forming ability and brittleness, which may be due to the low molecular weight.[39] However, the PLLA/PCL multiblock copolymer not only has good film-forming property, but also can undergo bending, twisting and tensile deformations, indicating that it has good toughness. Therefore, the flexible PLLA/PCL multiblock copolymer may be able to promote the degree of stereocomplexation of sc-PLA. Further, the modification of the synthesized multiblock copolymer for sc-PLA was discussed.

3.3. Crystallization and melting behaviors of sc-PLA/MBC blends

Fig. 4 shows WAXD patterns of sc-PLA and sc-PLA/MBC blends. For sc-PLA blend, there exhibits several obvious diffraction peaks at about 12.0°, 16.9°, 18.9°, 20.7° and 24.0°. The peaks at 12.0°, 20.7° and 24.0° are attributed to the (110), (300)/(030) and (220) planes of stereocomplex crystals (sc-crystals).[40] The peaks at 16.9° and 18.9° are assigned to the (110)/(200) and (203) planes of homo-crystallization crystals (hc-crystals).[36,40] In Fig. 4(a), with increasing of the MBC content, the intensity of the diffraction peaks corresponded to the sc-crystals first increases and then decreases, but the diffraction peaks of hc-crystals doesn't show a significant change. The possible reason is that although stereocomplex crystallization is stronger than homo-crystallization, both stereocomplex crystallization and homo-crystallization occur during solution casting, causing

mutual interference. This phenomenon is consistent with the results of the DSC 1st heating curves in the ESI (Fig. S3†). Fig. 4(b) shows WAXD patterns of sc-PLA/MBC blends with different MBC. It is clear that all blends show similar diffraction peaks including sc-crystals and hc-crystals. This indicates that the composition of MBC has no significant effect on the fully stereocomplexation of sc-PLA/MBC blends during solution casting. The possible reason is that the polymer chains in the solution have good mobility, so it is easy to arrange them to form hc-crystals and sc-crystals at the same time.

DSC cooling and reheating curves of sc-PLA/MBC blends are shown in Fig. 5, and the obtained thermal parameters are listed in Table S1.† In Fig. 5(a), the cooling curve of sc-PLA exhibits an exothermic peak at 125.2 °C, assigned to the stereocomplex crystallization between PLLA and PDLA. The corresponding reheating curve has an endothermic peak at 210.4 °C (Fig. 5(b)), corresponded to the melting of sc-crystals. A weaker melting peak is detected at 167.3 °C, which is attributed to the melting of PLA hc-crystals. This indicates that the stereocomplex crystallization is accompanied by homo-crystallization in the process of melting crystallization, which is because the high viscosity of the molten system limits the movement and regular arrangement of polymer chains. And the sc-crystals formed at higher temperature during the cooling process can be used as the heterogeneous nucleating agent to promote the homo-crystallization of PLLA or PDLA (as Fig. 1(b)). It is clear that only stereocomplex crystallization and its melting are observed on the DSC cooling curves when MBC is introduced, revealing that sc-PLA/MBC blends have achieved full stereocomplexation. This may be because the synthesized PLLA/PCL multi-block copolymer contains the soft PCL blocks, which endows PLLA/PCL multiblock copolymer with good mobility. This is conducive to the alternate arrangement of PLLA and PDLA segments to form PLA stereocomplex. With increasing of the MBC content from 0% to 15%, stereocomplex-crystallization temperature decreases from 125.2 °C to 95.2 °C. However, at 20% MBC, the crystallization peak has shifted to a higher temperature region (116.2 °C). The stereocomplex melting temperature of sc-PLA/MBC blends is significantly lower than that of sc-PLA, and the melting temperature first increases and then decreases as the MBC content increases. For sc-PLA/MBC blends with higher
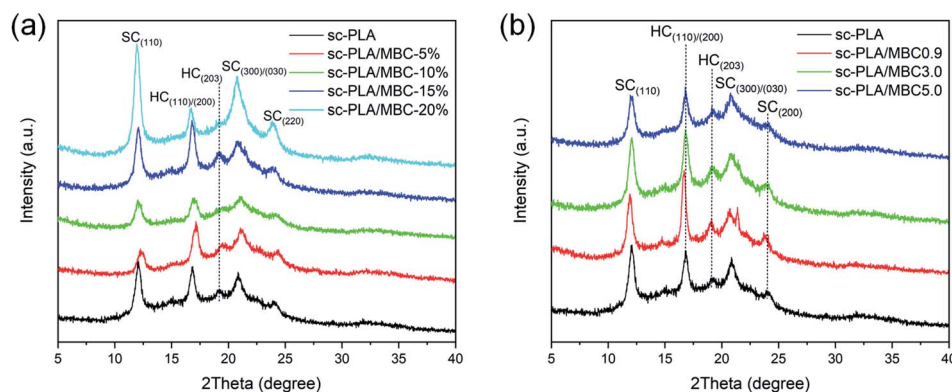

Fig. 4 WAXD patterns of sc-PLA and sc-PLA/MBC blends: (a) the blends with various MBC contents; (b) the blends with different MBC.
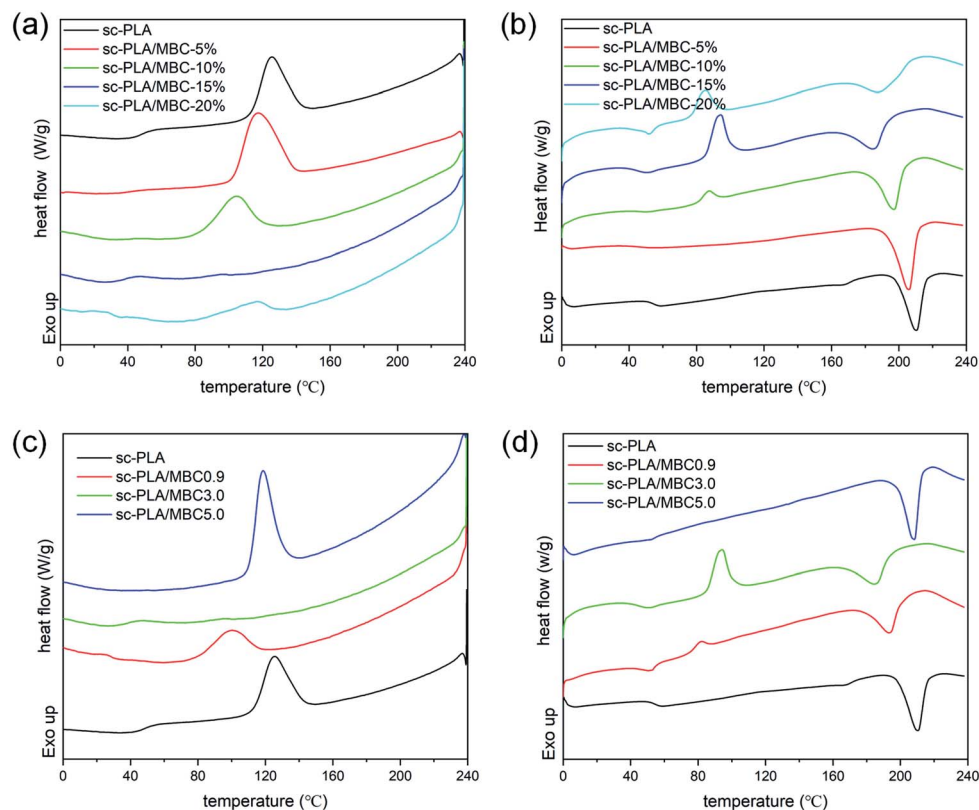
Fig. 5 DSC cooling (a and c) and reheating (b and d) of sc–PLA and sc–PLA/MBC blends: (a and b) the blends with various MBC contents; (c and d) the blends with different MBC.

MBC content ($\geq$10%), the cold crystallization peak is also observed in the low temperature region (80–110 °C). For the blend with 5% of MBC, the melting enthalpy of stereocomplex crystals is 34.2 J g^{-1}, which is larger than that of sc-PLA (as listed in Table S1†). With the increase of MBC content, the melting enthalpy of stereocomplex crystals shows a decreasing trend. These results reveal that the PLLA/PCL multi-block copolymer exhibits the duality for the crystallization of sc-PLA. The PCL block in the multi-block copolymer acts as the plasticizer to limit the polymer crystallization. But the soft PCL block promotes the movement of PLLA and PDLA chains, which is conducive to the alternating arrangement of PLLA and PDLA to produce stereocomplex crystallization. Similar result has been reported in PLLA/PDLA-*b*-PEG-*b*-PDLA blends.[41]

In Fig. 5(c), as the molecular weight of PLLA block in the multi-block copolymer increases, the temperature and enthalpy corresponded to the stereocomplex crystallization peak first decrease and then increase. The reheating curve of sc-PLA/MBC0.9 blend exhibits an cold crystallization peak at 81.6 °C, as displayed in Fig. 5(d). For sc-PLA/MBC3.0 blend, the cold crystallization peak shifts a higher temperature region (97.1 °C) and exhibits a larger enthalpy value (20.3 J g^{-1}). However, the cold crystallization peak of sc-PLA/MBC blends is not detected. It is clear in Table S1† that as the PLLA block in the multi-block copolymer increases, the melting temperature and enthalpy both increase first and then decrease. These results reveal that the composition of MBC affects the crystallization and melting

behaviors of sc-PLA. The increased molecular weight of the PLLA block leads to a decrease in the mobility of the multi-block copolymer and PLA, which is not conducive to the regularity of the polymer segment in the crystal lattice. And the increased molecular weight of PLLA blocks results in the more entanglement between the polymer chains, which promotes homogeneous nucleation of PLLA or PDLA. These results indicate that the synthesized multi-block copolymer acts as a compatibilizer to stabilize the regular PLLA/PDLA chain clusters in the melt blends (as Fig. 1(b)), thereby promoting the exclusive formation of sc-crystals in the melt-processed blend products.[18]

3.4. Nucleation and crystal growth during isothermal crystallization

Fig. 6 shows POM images of sc-PLA and sc-PLA/MBC blends with various MBC contents. For sc-PLA, small spherulites can be observed by isothermal crystallization at 180 °C for 5 min. With increasing of the isothermal crystallization time, the spherulites become larger and exhibit remarkable Maltese crosses. This is assigned to the orientation of sc-lamella along the radial direction. When MBC is introduced into the matrix, spherulites can be observed with naked eyes after 3 min of isothermal crystallization. However, with further increasing of the MBCs content, the isothermal crystallization time required for observing spherulites becomes longer. It can be observed that the sc-PLA/MBC blends with higher MBC content, spherulites
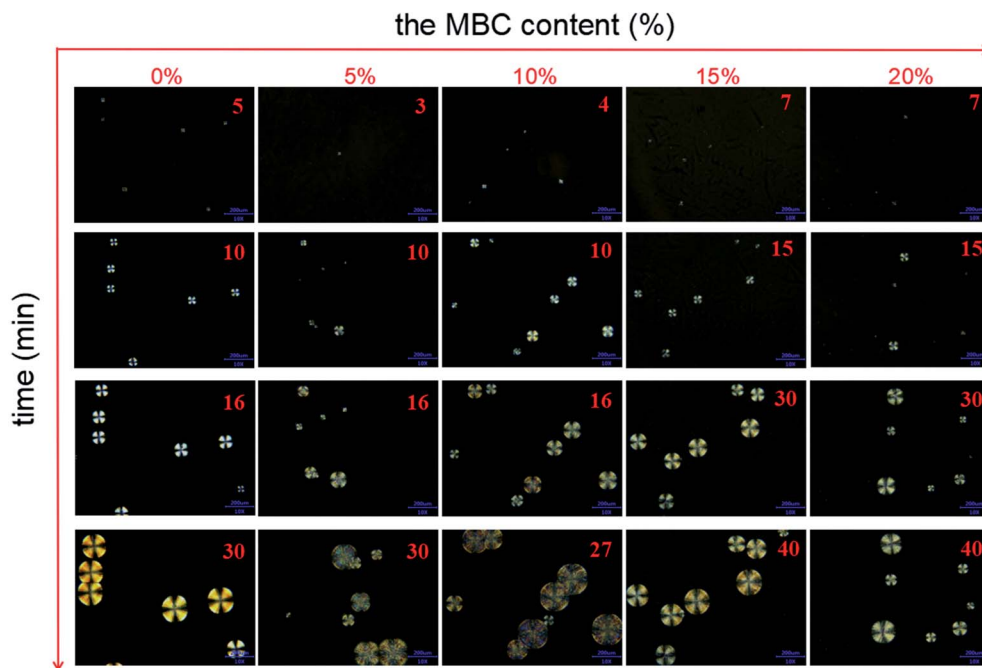
Fig. 6 POM photos of sc-PLA and sc-PLA/MBC blends with various MBC contents during isothermal crystallization of 180 °C.

show a smaller growth rate, and the density of spherulites increases as the isothermal crystallization time increases. These results reveal that the PLLA/PCL multiblock copolymer inhibits the homogeneous nucleation of the stereocomplex crystallization between PLLA and PDLA. The selected isothermal crystallization temperature is higher than the melting temperature of PCL block, so PCL block is in a molten state. The molten PCL block not only endows the PLLA/PCL multiblock copolymer with good motility, but also promotes the motility of PLLA and PDLA. The good mobility of polymer chains is not conducive to the formation of homogeneous nucleating agents from polymer collisions.

The effect of the composition of MBC on the nucleation and crystal growth was analyzed, as shown in Fig. S4.† For sc-PLA/MBC0.9 blends, the isothermal crystallization time required for observing spherulites takes a long time (6 min), and there exhibits a low spherulite density. This further confirms that the presence of molten PCL as the diluent is not conducive to the homogeneous nucleation of PLA enantiomers.[42] As the molecular weight of the PLLA block of the PCL/PLLA multi-block copolymer increases, the spherulite density increases significantly. The larger molecular weight of the PLLA block reduces the mobility the polymer, which can increase the effective collision between polymer chains, thereby promoting the homogeneous nucleation of the polymer chains.[43] The effect of isothermal crystallization temperature on nucleation and crystal growth are also discussed, as displayed in Fig. 7. At 170 °C, the significant spherulites can be observed in about 2 min. As the isothermal crystallization temperature increases, the time required for the first observation of spherulites increases, indicating that the increased crystallization temperature makes it more difficult to form homogeneous nucleation

sites for stereocomplex crystals. However, when the isothermal crystallization temperature is 185 °C and 190 °C, the spherulites have a larger radius in same crystallization time. It can be also observed that with increasing of the isothermal crystallization temperature, the density of spherulites decreases and the difference in spherulites size becomes more significant. The formation of spherulites includes two stages: nucleation and crystal growth. The lower temperature is conducive to homogeneous nucleation, resulting in a high spherulite density. The higher temperature accelerates the movement of the polymer chain, leading to a prolonged induction period of homogeneous nucleation and a faster spherulite growth rate.[44,45]

3.5. Thermal stability

Thermal stability of sc-PLA/MBCs blends are reflected in the change of the onset temperature of degradation ($T_{5 \text{ wt\%}}$) and degradation temperature (T_d). In Fig. 8, thermal degradation of the blends occurs in two steps. It is already well known that PLLA degrades at lower temperatures than PCL.[46] So, the PLA is first degraded, and then the PCL is degraded. And the introduction of PCL/PLLA multi-block copolymer in the blend can result in a decrease in the overall thermal stability of the material, which may be because the PLLA/PCL multi-block copolymer presents a lower thermostability compared with PLA (as shown in Fig. 3(d)). The substances produced by the degradation of multi-block copolymer may accelerate the degradation of PLA. As listed in Table S2,† the higher content of MBCs (10–20 wt%) shifts the $T_{5\%}$ of the material to a lower temperature value by around 10 °C, and the significant shift to lower value (270–273 °C) was also observed for maximum degradation temperature. With increasing of molecular weight of PLLA block in the multi-block copolymer, the values of $T_{5\%}$
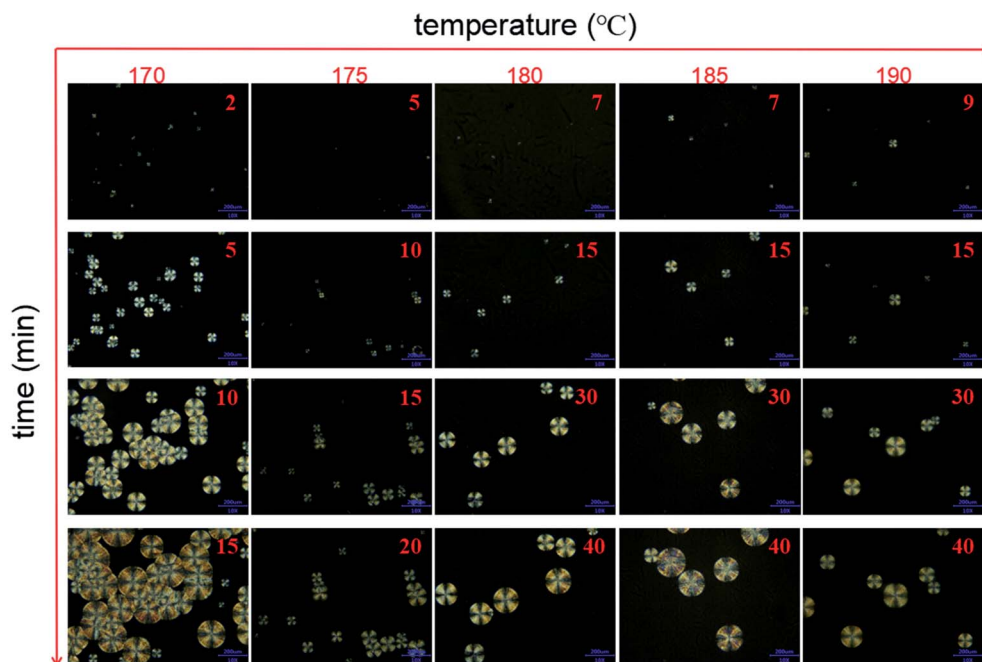
Paper

Fig. 7 POM photos of isothermal crystallization of sc–PLA/MBC–15% blends at various temperatures.
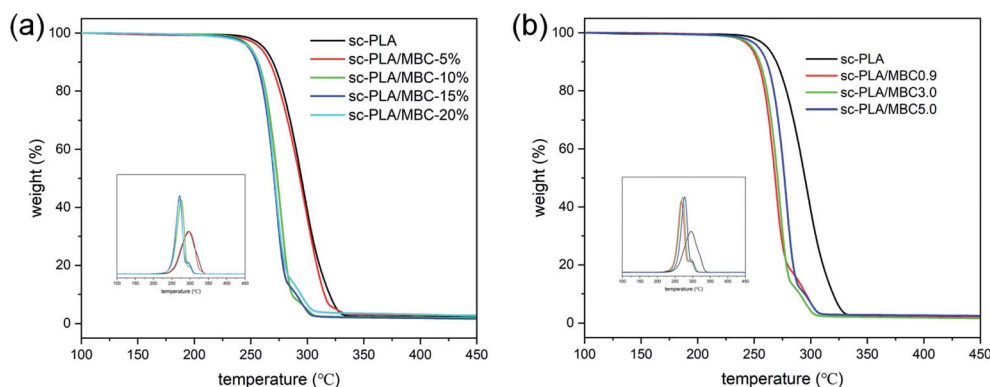

Fig. 8 TGA curves of sc–PLA and sc–PLA/MBC blends: (a) the blends with various MBC contents; (b) the blends with different MBC.

and T_d increase, as shown in Fig. 8(b) and Table S2.† This is attributed to the higher molecular weight of PLLA blocks, which has also been demonstrated by Takenaka et al.[47]

3.6. Mechanical properties

Mechanical properties of sc-PLA and sc-PLA/MBC blends were evaluated, and the obtained results are presented in Fig. 9. It is clearly observed from Fig. 9(a) that the tensile strength and elongation at break are significantly influenced by the MBC content. For sc-PLA, the tensile strength and elongation at break are 69.5 MPa and 16.4%, respectively. The increase in MBC content is found to cause a slight decrease in the tensile strength, while the increase of the elongation at break can be observed, as displayed in Fig. 9(b). The tensile strength and elongation at break changes significantly (39.3 MPa and 189%) when the MBC content exceeds 15%. This indicates that the fracture behavior of

the sample in the tensile test changed from the brittleness of pure sc-PLA to the ductile fracture of sc-PLA/MBC-20% blends, which is ascribed to the intrinsic high flexibility of the PLLA/PCL multi-block copolymer. Similar phenomena have been reported by Zhang et al.[48] and Xiao et al.[49] Considering the loss in tensile strength accompanied by the multi-block copolymer, the appropriate contents of the multi-block copolymer should be 10–15% in the sc-PLA/MBC blends.

The effect of different MBC on the mechanical properties of the sc-PLA/MBC blends were also discussed, as shown in Fig. 9(c) and (d). Compared to sc-PLA, tensile strength of sc-PLA/MBC blends decreases, and their elongation at break increases. This is mainly attributed to the toughening of sc-PLA blends by PLLA/PCL multi-block copolymer. A slight increment of tensile strength of sc-PLA/MBC blends could be observed with increase in the PLLA block length of the multi-block copolymer MBC,
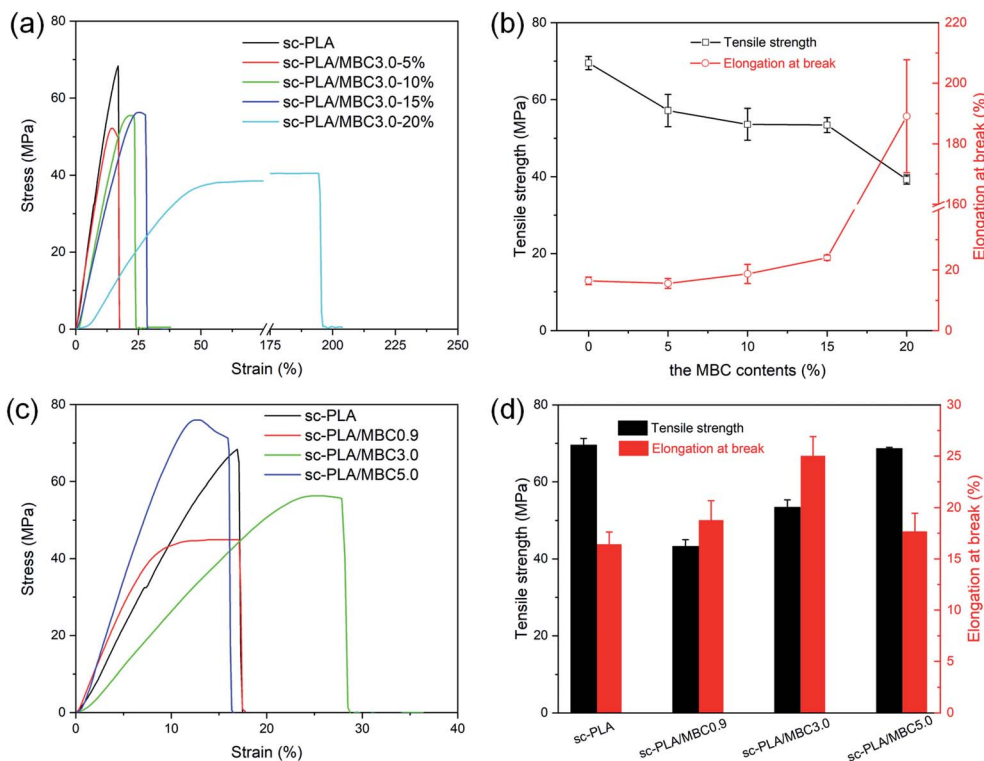
Fig. 9 Tensile stress–strain curves (a and c) of sc–PLA and sc–PLA/MBC blends and the corresponding tensile strength and elongation at break (b and d): (a and b) the blends with various MBC; (c and d) the blends with different MBC.

which can be seen as the synergistic effect of molecular of PLLA/PCL multi-block copolymer and stereocomplexation. Because the molecular weight of the synthesized multi-block copolymer is much lower than that of PLLA and PDLA, the increased PLLA block increases the molecular weight of multi-block copolymer, thereby improving the tensile strength of sc-PLA/MBC blends. At the same time, the increased PLLA block promotes the stereocomplexation between PLLA and PDLA, which results in higher tensile strength. As for the elongation at break, it first increases and then decreases as the length of the PLLA block of MBC increases. When the multi-block copolymer MBC with shorter PLLA block is added, the increase in elongation at break could be attributed to the fact that the critical amount of PCL content is reached. However, with further longer of PLLA block, the elongation at break decreases, which may be due to the physical cross-linking effect of a large number of the formed stereocomplexes that restricts the movement of the polymer chains.[50]

4. Conclusions

In this research, the flexible PLLA/PCL multi-block copolymers based on self-complementary quadruple hydrogen bonds were synthesized and characterized. The influences of the PLLA/PCL multi-block copolymers on the crystallization, nucleation, thermal stability and mechanical properties of sc-PLA were investigated. The results revealed that the PLLA/PCL multi-block copolymers promoted the stereocomplexation of the

PLA enantiomers during the melting crystallization process to obtain a complete stereocomplexed material, and can also improve the brittleness of sc-PLA. DSC and POM results found that the PCL block leads to a decrease in the melting temperature of stereocomplex and difficulty in homogeneous nucleation, which may be attributed to the plasticizing effect of PCL. The results revealed that this study proposes a new method for the preparation of fully stereocomplexed tough PLA-based materials.

Conflicts of interest

The authors declare no conflicts of interest.

Acknowledgements

References

1 L. Genovese, M. Soccio, N. Lotti, M. Gazzano, V. Siracusa, E. Salatelli, F. Balestra and A. Munari, *Eur. Polym. J.*, 2017, **95**, 289.

2   I. D'Auria, M. C. D'Alterio, C. Tedesco and C. Pellecchia, *RSC Adv.*, 2019, **9**, 32771.

3   X. Zhou, J. Deng, C. Fang, W. Lei, Y. Song, Z. Zhang, Z. Huang and Y. Li, *J. Mater. Sci. Technol.*, 2021, **60**, 27.

4   S. Moradi and J. K. Yeganeh, *Polym. Test.*, 2020, **91**, 106735.

5   V. Izraylit, M. Heuchel, O. E. C. Gould, K. Kratz and A. Lendlein, *Polymer*, 2020, **209**, 122984.

6   X. Cao, Y. Wang, H. Chen, J. Hu and L. Cui, *Composites, Part B*, 2021, **217**, 108934.

7   B. Palai, S. Mohanty and S. K. Nayak, *Polym. Test.*, 2020, **83**, 106130.

8   M. Naddeo, A. Sorrentino and D. Pappalardo, *Polymers*, 2021, **13**, 627.

9   J. Bao, X. Dong, S. Chen, W. Lu, X. Zhang and W. Chen, *Polymer*, 2020, **190**, 122189.

10 B. Ma, H. Zhang, K. Wang, H. Xu, Y. He and X. Wang, *Compos. Commun.*, 2020, **21**, 100380.

11 N. D. Tien and R. E. Prud'homme, *Polymer*, 2017, **117**, 25.

12 S. Saeidlou, M. A. Huneault, H. Li, P. Sammut and C. B. Park, *Polymer*, 2012, **53**, 5816.

13 T. Lv, J. Li, S. Huang, H. Wen, H. Li, J. Chen and S. Jiang, *Polymer*, 2021, **222**, 123648.

14 A. K. Pandey, H. Takagi, N. Igarashi, N. Shimizu and S. Sakurai, *Polymer*, 2021, **229**, 124001.

15 L. Cui, Y. Wang, R. Zhang and Y. Liu, *Adv. Polym. Technol.*, 2018, **37**, 2429.

16 S. Deng, H. Bai, Z. Liu, Q. Zhang and Q. Fu, *Macromolecules*, 2019, **52**, 1718.

17 N. Mulchandani, A. Gupta, K. Masutani, S. Kumar, S. Sakurai, Y. Kimura and V. Katiyar, *ACS Appl. Polym. Mater.*, 2019, **1**, 3354.

18 S. Deng, J. Yao, H. Bai, H. Xiu, Q. Zhang and Q. Fu, *Polymer*, 2021, **224**, 123736.

19 H. Tsuji, K. Iguchi and Y. Arakawa, *Polymer*, 2021, **213**, 123226.

20 H. Liu, W. Zhou, P. Chen, D. Bai, Y. Cai and J. Chen, *Polymer*, 2020, **210**, 122873.

21 Y. Liu, J. Shao, J. Sun, X. Bian, Z. Chen, G. Li and X. Chen, *Mater. Lett.*, 2015, **155**, 94.

22 S. R. Rathi, E. B. Coughlin, S. L. Hsu, C. S. Golub, G. H. Ling and M. J. Tzivanis, *Polymer*, 2012, **53**, 3008.

23 H. Wang, J. Yu, H. Fang, H. Wei, X. Wang and Y. Ding, *Polymer*, 2018, **137**, 1.

24 P. Purnam, Y. Jung and S. H. Kim, *Macromolecules*, 2012, **45**, 4012.

25 Y. Liu, J. Shao, J. Sun, X. Bian, L. Feng, S. Xiang, B. Sun, Z. Chen, G. Li and X. Chen, *Polym. Degrad. Stab.*, 2014, **101**, 10.

26 B. J. B. Folmer, R. P. Sijbesma, R. M. Versteegen, J. A. J. van der Rijt and E. W. Meijer, *Adv. Mater.*, 2000, **12**, 874.

27 Z. Jing, X. Shi, G. Zhang and J. Gu, *Polymer*, 2017, **121**, 124.

28 Y. Ren, Z. Z. Zhang, W. Xia, Q. Zhou and X. Sun, *Eur. Polym. J.*, 2021, **147**, 110252.

29 D. Caner, E. Doganci, M. D. Doganci and G. Ozkoc, *J. Mech. Behav. Biomed. Mater.*, 2021, **122**, 104656.

30 C. Yan, Y. P. Jiang, D. F. Hou, W. Yang and M. B. Yang, *Polymer*, 2020, **186**, 122021.

31 Z. Uyar, M. Durgun, M. S. Yavuz, M. B. Abaci, U. Arslan and M. Degirmenci, *Polymer*, 2017, **123**, 153.

32 W. Lee, S. Y. Kwak and J. W. Chung, *Eur. Polym. J.*, 2020, **138**, 109976.

33 R. Chang, Y. Huang, G. Shan, Y. Bao, X. Yun, T. Dong and P. Pan, *Polym. Chem.*, 2015, **6**, 5899.

34 C. Chen, X. W. Zhang and H. M. Ye, *Crystals*, 2021, **11**, 1530.

35 P. Kotcharat, P. Chuysinuan, T. Thanyacharoen, S. Techasakul and S. Ummartyotin, *Sustainable Chem. Pharm.*, 2021, **20**, 100404.

36 S. J. Sheng, X. Hu, F. Wang, Q. Y. Ma and M. F. Gu, *Mater. Sci. Eng., C*, 2015, **49**, 612.

37 V. Vilay, M. Mariatti, Z. Ahmad, K. Pasomsouk and M. Todo, *Mater. Sci. Eng., A*, 2010, **527**, 6930.

38 I. Navarro-Baena, J. M. Kenny and L. Peponi, *Polym. Degrad. Stab.*, 2014, **108**, 140.

39 I. Lee, T. R. Panthani and F. S. Bates, *Macromolecules*, 2013, **46**, 7387.

40 T. Lv, J. Li, S. Huang, H. Wen, H. Li, J. Chen and S. Jiang, *Polymer*, 2021, **222**, 123648.

41 Y. Song, D. Wang, N. Jiang and Z. Gan, *ACS Sustainable Chem. Eng.*, 2015, **3**, 1492.

42 L. Li, Z. Q. Cao, R. Y. Bao, B. H. Xie, M. B. Yang and W. Yang, *Eur. Polym. J.*, 2017, **97**, 272.

43 H. Tsuji, T. Wada, Y. Sakamoto and Y. Sugiura, *Polymer*, 2010, **51**, 4937.

44 Y. Feng, P. Lv, L. Jiang, P. Ma, M. Chen, W. Dong and Y. Chen, *Polym. Degrad. Stab.*, 2017, **146**, 113.

45 J. Bao, X. Dong, S. Chen, W. Lu, X. Zhang and W. Chen, *Polymer*, 2020, **190**, 122189.

46 I. Navarro-Baena, J. M. Kenny and L. Peponi, *Polym. Degrad. Stab.*, 2014, **108**, 140.

47 M. Takenaka, Y. Kimura and H. Ohara, *Polymer*, 2018, **155**, 218.

48 B. Zhang, X. Bian, S. Xiang, G. Li and X. Chen, *Polym. Degrad. Stab.*, 2017, **136**, 58.

49 X. Xiao, V. S. Chevali, P. Song, B. Yu, Y. Yang and H. Wang, *Compos. Commun.*, 2020, **21**, 100385.

50 Y. Liu, J. Shao, J. Sun, X. Bian, L. Feng, S. Xiang, B. Sun, Z. Chen, G. Li and X. Chen, *Polym. Degrad. Stab.*, 2014, **101**, 10–17.